

## Kinetic Analysis of Bio-Oil Aging by Using Pattern Search Method

Shukai Zhang, Chong Li, Xiaojuan Guo, Md. Maksudur  
Rahman, Xingguang Zhang, Xi Yu, and Junmeng Cai

*Ind. Eng. Chem. Res.*, **Just Accepted Manuscript** • DOI: 10.1021/acs.iecr.9b05629 • Publication Date (Web): 02 Jan 2020

Downloaded from pubs.acs.org on January 6, 2020

### Just Accepted

“Just Accepted” manuscripts have been peer-reviewed and accepted for publication. They are posted online prior to technical editing, formatting for publication and author proofing. The American Chemical Society provides “Just Accepted” as a service to the research community to expedite the dissemination of scientific material as soon as possible after acceptance. “Just Accepted” manuscripts appear in full in PDF format accompanied by an HTML abstract. “Just Accepted” manuscripts have been fully peer reviewed, but should not be considered the official version of record. They are citable by the Digital Object Identifier (DOI®). “Just Accepted” is an optional service offered to authors. Therefore, the “Just Accepted” Web site may not include all articles that will be published in the journal. After a manuscript is technically edited and formatted, it will be removed from the “Just Accepted” Web site and published as an ASAP article. Note that technical editing may introduce minor changes to the manuscript text and/or graphics which could affect content, and all legal disclaimers and ethical guidelines that apply to the journal pertain. ACS cannot be held responsible for errors or consequences arising from the use of information contained in these “Just Accepted” manuscripts.

## Kinetic Analysis of Bio-Oil Aging by Using Pattern Search Method

Shukai Zhang <sup>1</sup>, Chong Li <sup>1</sup>, Xiaojuan Guo <sup>2,\*</sup>, Md. Maksudur Rahman <sup>1</sup>, Xingguang Zhang <sup>3</sup>, Xi Yu <sup>4</sup>, Junmeng Cai <sup>1,\*</sup>

<sup>1</sup> Biomass Energy Engineering Research Center, School of Agriculture and Biology, Shanghai Jiao Tong University, 800 Dongchuan Road, Shanghai 200240, People's Republic of China

<sup>2</sup> School of Chemical Engineering and Energy Technology, Dongguan University of Technology, 1 Daxue Road, Songshan Lake, Dongguan 523808, Guangdong Province, People's Republic of China

<sup>3</sup> Department of Chemistry, School of Science, University of Shanghai for Science and Technology, 516 Jungong Road, Shanghai 200093, People's Republic of China

<sup>4</sup> Energy & Bioproducts Research Institute, Aston University, Aston Triangle, Birmingham B4 7ET, United Kingdom

\* Corresponding authors: Xiaojuan Guo. E-mail: guoxj@dgut.edu.cn; Junmeng Cai.

E-mail: jmcai@sjtu.edu.cn

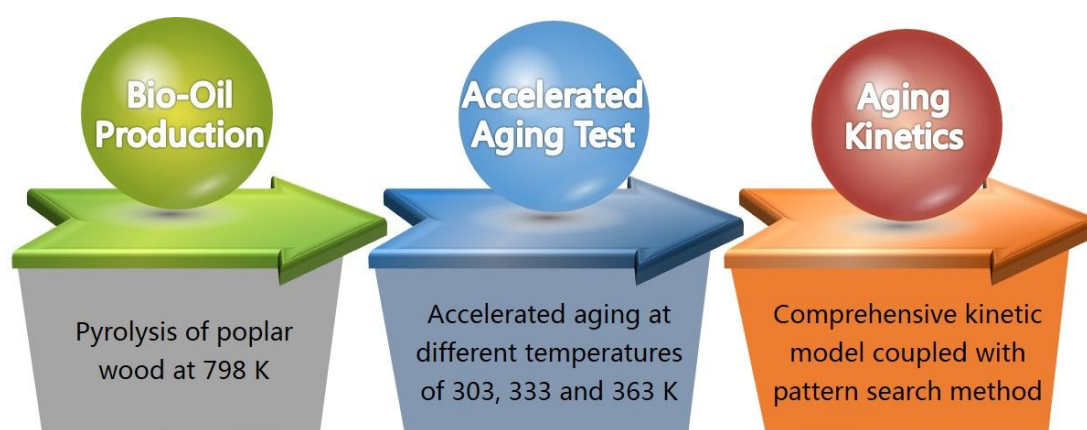
### Abstract

Bio-oil derived from fast pyrolysis of lignocellulosic biomass is unstable, and aging would occur during its storage, handling, and transportation. The kinetic analysis of bio-oil aging is fundamental for the investigation of bio-oil aging mechanisms and

1  
2  
3  
4 the utilization of bio-oil as bio-fuels, bio-materials or bio-chemicals. The aging kinetic  
5  
6  
7 experiments of bio-oil from poplar wood pyrolysis were conducted at different aging  
8  
9  
10 temperatures of 303, 333, 353 and 363 K for different specified periods of time in  
11  
12 capped glass vessels. The traditional method with two separated fittings was employed  
13  
14 to fit experimental data, and the results indicated that the obtained kinetic parameters  
15  
16 could not fit the experimental data well. An advanced approach for kinetic modeling of  
17  
18 bio-oil aging has been developed by simultaneously processing experimental data at  
19  
20 different aging temperatures and using the pattern search method. The aging kinetic  
21  
22 model with the optimized parameters predicted the aging kinetic experimental data of  
23  
24 the bio-oil sample very well for different aging temperatures.  
25  
26  
27  
28

29  
30 **Keywords:** Bio-Oil; Aging Kinetics; Viscosity; Weight-Average Molecular Weight;  
31  
32 Pattern Search Method  
33  
34  
35  
36  
37

### 38 Graphical abstract



### 57 1 Introduction

58  
59 China is facing the shortage of liquid fuels which are mainly derived from  
60

1  
2  
3  
4 petroleum <sup>1, 2</sup>. Bio-oil from biomass pyrolysis can be utilized as a promising  
5  
6 intermediate for producing transportation fuels to replace petroleum-derived liquid  
7  
8 fuels <sup>3</sup>. Bio-oil contains a considerable amount of oxygen due to the presence of  
9  
10 oxygenated compounds, which results in a low energy density <sup>4</sup>. It contains relatively  
11  
12 little sulfur and nitrogen <sup>5</sup>. While crude oil composes of hydrocarbon deposits and other  
13  
14 organic materials and contains an amount of sulfur, which is an undesirable  
15  
16 contaminant because it generates sulfur oxides when burned <sup>6</sup>. Bio-oil has some certain  
17  
18 advantages when it is used as a biofuel <sup>7-9</sup>: (1) cost efficiency, (2) easy excess to source,  
19  
20 (3) renewability, (4) greenhouse gases reduction, (5) economic security, and (6)  
21  
22 reduction of reliance on foreign oil. And the bio-oil heavy fraction has similar  
23  
24 components and physicochemical properties as bitumen, such as saturated, aromatic  
25  
26 and polar compounds as well as asphaltene <sup>10</sup>. Therefore, the utilization of bio-oil as a  
27  
28 bio-asphalt or an additive for asphalt becomes very promising <sup>10-13</sup>.

29  
30  
31  
32  
33  
34  
35  
36  
37  
38 However, bio-oil is chemically and thermally unstable during storage, handling,  
39  
40 and transportation, which limits the utilization of bio-oil <sup>14-16</sup>. Aged bio-oil typically  
41  
42 shows phase separation, increased viscosity, average molecular weight and water  
43  
44 content <sup>17</sup>. The aging phenomena are mainly caused by the evaporation of light volatile  
45  
46 components, and the condensation, polymerization, esterification and oxidative  
47  
48 reactions occurring among bio-oil components <sup>18</sup>.

49  
50  
51  
52  
53 From the literature review, most recent studies on bio-oil aging were related to  
54  
55 investigating aging process parameter effects, characterizing changes in  
56  
57 physicochemical properties of bio-oils and seeking approaches to slow down the aging  
58  
59  
60

1  
2  
3  
4 rate of bio-oils <sup>16, 17</sup>.

5  
6 The comprehensive understanding on bio-oil aging kinetics is helpful to determine  
7 the aging rate and the important properties of bio-oil under different aging periods, and  
8  
9 predict the required time to reach different degrees of aging, which is important for the  
10 application of bio-oil as a bio-fuel, bio-chemical or bio-material and for the efficiency  
11 verification of various approaches to slow down bio-oil aging rate <sup>19, 20</sup>. The aging  
12 kinetic parameters including aging activation energy and frequency factor obtained  
13 from the kinetic modeling of bio-oil aging are very important for the quantitative  
14 interpretation of bio-oil aging behaviors <sup>21</sup>. The aging activation energy can be used to  
15 evaluate the performance for asphalt <sup>22</sup>, since bio-oil has the possibility to use as an  
16 asphalt substitute <sup>23, 24</sup>.

17  
18  
19  
20  
21  
22  
23  
24  
25  
26  
27  
28  
29  
30  
31  
32  
33  
34  
35  
36  
37  
38  
39  
40  
41  
42  
43  
44  
45  
46  
47  
48  
49  
50  
51  
52  
53  
54  
55  
56  
57  
58  
59  
60  
Several studies were carried out on the kinetic modeling of bio-oil aging <sup>25-27</sup>. In  
those studies, an exponential equation was generally used to describe the change in bio-  
oil's properties with respect to aging time, and the effect of other factors on aging was  
not considered. And the corresponding kinetic method for bio-oil aging is unable to  
provide accurate aging kinetic parameters, which will be discussed in detail later.

The main aim of this paper is to investigate the aging behaviors of bio-oil from  
poplar wood pyrolysis and to develop an advanced procedure for kinetic modeling of  
bio-oil aging.

## 2 Experiments and analytical methods

The bio-oil samples were obtained from poplar wood pyrolysis at 798 K in a  
fluidized-bed reactor with a capacity of 5 kg h<sup>-1</sup>. The experimental setup for the

1  
2  
3  
4 production of bio-oil was described in detail in an earlier publication <sup>28</sup>. The collected  
5  
6 liquid contained some quench medium and water. The collected liquid was centrifuged  
7  
8 for 30 minutes at 4000 rpm in order to remove them <sup>29</sup>. After centrifugation, the bio-oil  
9  
10 samples were immediately placed in capped glass vessels at atmospheric pressure and  
11  
12 then stored in a forced-air oven <sup>30</sup>. The bio-oil samples were stored at the aging  
13  
14 temperatures of 303, 333, 353, and 363 K for 90 days, 10 days, 60 hours and 24 hours,  
15  
16 respectively. The pH value, water content, viscosity, average molecular weight, higher  
17  
18 heating value (HHV) of the fresh and aged bio-oil sample were measured. The tests  
19  
20 were repeated in triplicate and the average value was used for further analysis. Some  
21  
22 experimental data will be used to estimate the aging kinetic parameters, and the other  
23  
24 experimental data will be used to determine the validity of the aging kinetic model.  
25  
26  
27  
28  
29  
30  
31

32 The water content of the bio-oil sample was determined by Karl Fischer titration  
33  
34 in accordance with ASTM E203-08.. The bio-oil samples' pH values were determined  
35  
36 at room temperature using a digital pH probe (Accumet model 8250, Fisher Scientific)  
37  
38 in accordance with ASTM E70 - 07. The HHV of the bio-oil sample was obtained using  
39  
40 an oxygen bomb calorimeter (XRY-1B, Shanghai Changji Geological Instruments Co.,  
41  
42 Ltd., China) in accordance with ASTM E711-81. The bio-oil's viscosity was measured  
43  
44 using a rotational viscometer (Brookfield viscometer model DV- II + Pro, Ametek, Inc,  
45  
46 USA) in accordance with ASTM D2983 - 19.  
47  
48  
49  
50  
51  
52

53 The molecular weight and its distribution of the fresh and aged bio-oil samples  
54  
55 were analyzed using gel permeation chromatography (GPC, HLC-8321GPC/HT, Tosoh,  
56  
57 Japan) equipped with a refractive index (RI), an ultraviolet (UV) detector and a sample  
58  
59  
60

pretreatment system. Two Agilent PLgel columns (3 $\mu$ m 100 Å 300  $\times$  7.5 mm) and one Mesopore column (300  $\times$  7.5 mm) were coupled in series. Tetrahydrofuran (THF), a suitable solvent for the GPC analysis of bio-oil<sup>31</sup>, was used as the solvent at 1 mL min<sup>-1</sup>. The GPC analyses of bio-oil samples were performed in accordance with ASTM D6474 - 12. Before GPC analysis, each bio-oil sample was dissolved in THF and filtered using a 0.45- $\mu$ m syringe filter. All of the samples were found in the mobile phase (THF). When the molecular weight distribution is obtained, the average molecular weight can be calculated<sup>32, 33</sup>. In this study, the weight-average molecular weight was used:

$$MW = \frac{\sum_i w_i M_i}{\sum_i w_i} \quad (1)$$

where  $w_i$  and  $M_i$  are the weight fraction and molecular weight of the  $i$ -th component in bio-oil, respectively.

### 3 Traditional method for aging kinetic analysis

The common aging kinetic models are expressed in terms of change in viscosity with the form of exponential functions<sup>25, 27</sup>. The bio-oils contains many chemical compounds mainly including phenolic components, alcohols, acids, aldehydes, ketones, esters, anhydrosugars, furans and oligomers<sup>33, 34</sup>. The compositions and physicochemical properties of bio-oils are subject to change with aging time and temperature<sup>35</sup>. In addition to increased viscosity, aging can result in increasing average molecular weight, which indicates the average length of the bio-oil component's polymer chains<sup>33</sup>. According to previous studies<sup>36, 37</sup>, the aged bio-oil's weight-

average molecular weight shows a positive correlation with its viscosity.

According to the aging kinetic model based on the change in viscosity, the molecular weight based aging model can be obtained:

$$MW(t) = MW_0 + (MW_\infty - MW_0)[1 - \exp(-k \cdot t)] \quad (2)$$

In the above equation,  $t$  is the time,  $MW(t)$  is the weight-average molecular weight at the time  $t$ ,  $MW_0$  is the initial weight-average molecular weight,  $MW_\infty$  is the infinite time steady-state weight-average molecular weight, and  $k$  is the aging kinetic rate constant, which is dependent on the aging temperature<sup>38</sup>:

$$k = k_0 \exp\left(-\frac{E_a}{R \cdot T_a}\right) \quad (3)$$

where  $k_0$  is the pre-exponential factor of Arrhenius ( $s^{-1}$ ),  $E_a$  is the aging activation energy ( $J \text{ mol}^{-1}$ ),  $T_a$  is the aging temperature, and  $R$  is the universal gas constant ( $8.31452 \text{ J mol}^{-1} \text{ K}^{-1}$ ). In chemistry, the aging activation energy is the minimum quantity of energy which the reacting components must possess to initiate the aging reactions.

To perform the kinetic analysis of bio-oil aging, the parameters of the aging kinetic model including the  $MW_\infty$  values for different aging temperatures and the aging kinetic parameters  $k_0$  and  $E_a$  should be calculated. The traditional method for the estimation of the model parameters includes two separated fitting steps:

Step 1. Fitting Equation (2) to experimental data at each aging temperature and obtain  $k$  and  $MW_\infty$  values for each aging temperature;

Step 2. Fitting Equation (3) to resulting  $k_i$  vs.  $T_i$  ( $i = 1, \dots, n$ , where  $n$  is the number of aging temperatures considered) for different aging temperatures and obtain  $k_0$  and  $E_a$ .



Obviously, the first fitting step leads to some errors involved in  $k_i$  as the bio-oil aging kinetic model (Equation (2)) is an empirical model and it cannot describe the aging kinetic behaviors of bio-oils without any deviation, and the experimental data contain some measurement errors. The errors contained in the resulting parameters ( $k_i$ ) would be propagated when they will be used as the input data set in the second fitting step. The errors involved in the obtained aging kinetic parameters  $k_0$  and  $E_a$  would be amplified.

#### 4 Advanced procedure for aging kinetic analysis

To avoid the problem resulted from the traditional method, an alternative method is proposed in this study, which simultaneously considers the experimental data obtained at different aging temperatures.

Inserting Equation (3) in Equation (2) obtains the following equation:

$$MW(t) = MW_0 + (MW_\infty - MW_0) \left\{ 1 - \exp \left[ -k_0 \exp \left( -\frac{E_a}{R \cdot T_a} \right) \cdot t \right] \right\} \quad (4)$$

The above aging kinetic model describes the variation of weight-average molecular weight with the aging time and temperature.

The above model for bio-oil aging kinetics is applied simultaneously in order to adjust three  $MW - t$  curves at different aging temperatures. The estimation of the model parameter values and the investigation of the model quality are generally carried out by means of an objective function<sup>39</sup>, which usually uses the sum of the squared errors between the experimental data and model prediction:

$$\text{O.F.}(k_0, E_a, MW_{\infty,1}, MW_{\infty,2}, \dots) = \sum_{j=1}^{n_t} \sum_{i=1}^{n_{t,d}} (MW_{\text{exp},ij} - MW_{\text{cal},ij})^2 \quad (5)$$

1  
2  
3  
4 where  $MW_{exp}$  is the experimentally obtained weight-averaged molecular weight,  $MW_{cal}$   
5  
6 is the calculated weight-average molecular weight value obtained by numerical  
7  
8 calculation of Equation (4) with the given set of parameters, and the subscript  $i$  denotes  
9  
10 the  $i$ -th data point and the subscript  $j$  makes reference to a point in the  $j$ -th aging  
11  
12 temperature. From Equation (5), the experimental data at all aging temperatures were  
13  
14 considered in this study. When Equation (4) is solved using certain parameter values,  
15  
16 the  $MW_{cal}$  and then O.F. values can be calculated. The aging kinetic parameter values  
17  
18 can be obtained by minimizing the above objective function with some constraints:  
19  
20  
21  
22

$$23 \quad \min_p \text{O.F.}(p) \quad \text{subject to: } LB \leq p \leq UB \quad (6)$$

24  
25 where  $p$  is the vector of parameters including  $MW_{\infty}$  values at different aging  
26  
27 temperatures,  $k_0$  and  $E_a$ . LB and UB are lower and upper bound constraints for  $p$ ,  
28  
29 respectively.  
30  
31  
32  
33

34  
35 If the experimental data set at only one aging temperature would be used, the aging  
36  
37 kinetic parameters could be determined by using a common nonlinear fitting method.  
38  
39 When the experimental data sets at all aging temperatures are considered,  
40  
41 undetermined parameters include  $MW_{\infty,i}$  ( $i=1, \dots, n$ , where  $n$  is the aging  
42  
43 temperatures considered in this study),  $k_0$  and  $E_a$ , and the corresponding objective  
44  
45 function may cause some difficulties in the use of the common nonlinear fitting  
46  
47 method. In the present paper, the pattern search method is employed to solve the above  
48  
49 optimization problem. The method, as an optimization method, does not require  
50  
51 derivative information of the objective function<sup>40</sup>. The pattern search method is  
52  
53 commonly used in science and engineering to generate high-quality solutions to  
54  
55  
56  
57  
58  
59  
60

1  
2  
3  
4 optimize and search problems including parameter estimation of kinetic models  
5  
6 because of its advantages in robustness and function evaluations <sup>41, 42</sup>. The detailed  
7  
8 implementation of the pattern search method can found in the literature <sup>43</sup>. With each  
9  
10 set of parameters, the objective function values associated with the old and new  
11  
12 parameter sets are calculated. If the new parameter set reduces the function value, it is  
13  
14 accepted for the next iterative calculation. **Figure 1** depicts the block diagram of this  
15  
16 advanced procedure for bio-oil aging kinetic analysis.  
17  
18  
19  
20  
21

22  
23 Based on the above analyses, the advantages of the proposed advanced procedure  
24  
25 for bio-oil aging kinetic analysis can be summarized as follows: (1) the developed  
26  
27 comprehensive aging kinetic model considers the effect of both aging time and  
28  
29 temperature on aging kinetics; (2) the experimental data at all aging temperatures are  
30  
31 simultaneously used to perform the aging kinetic analysis; (3) the pattern search method  
32  
33 is used to determine the aging kinetic parameters.  
34  
35  
36  
37  
38  
39  
40  
41  
42  
43  
44  
45  
46  
47  
48  
49  
50  
51  
52  
53  
54  
55  
56  
57  
58  
59  
60

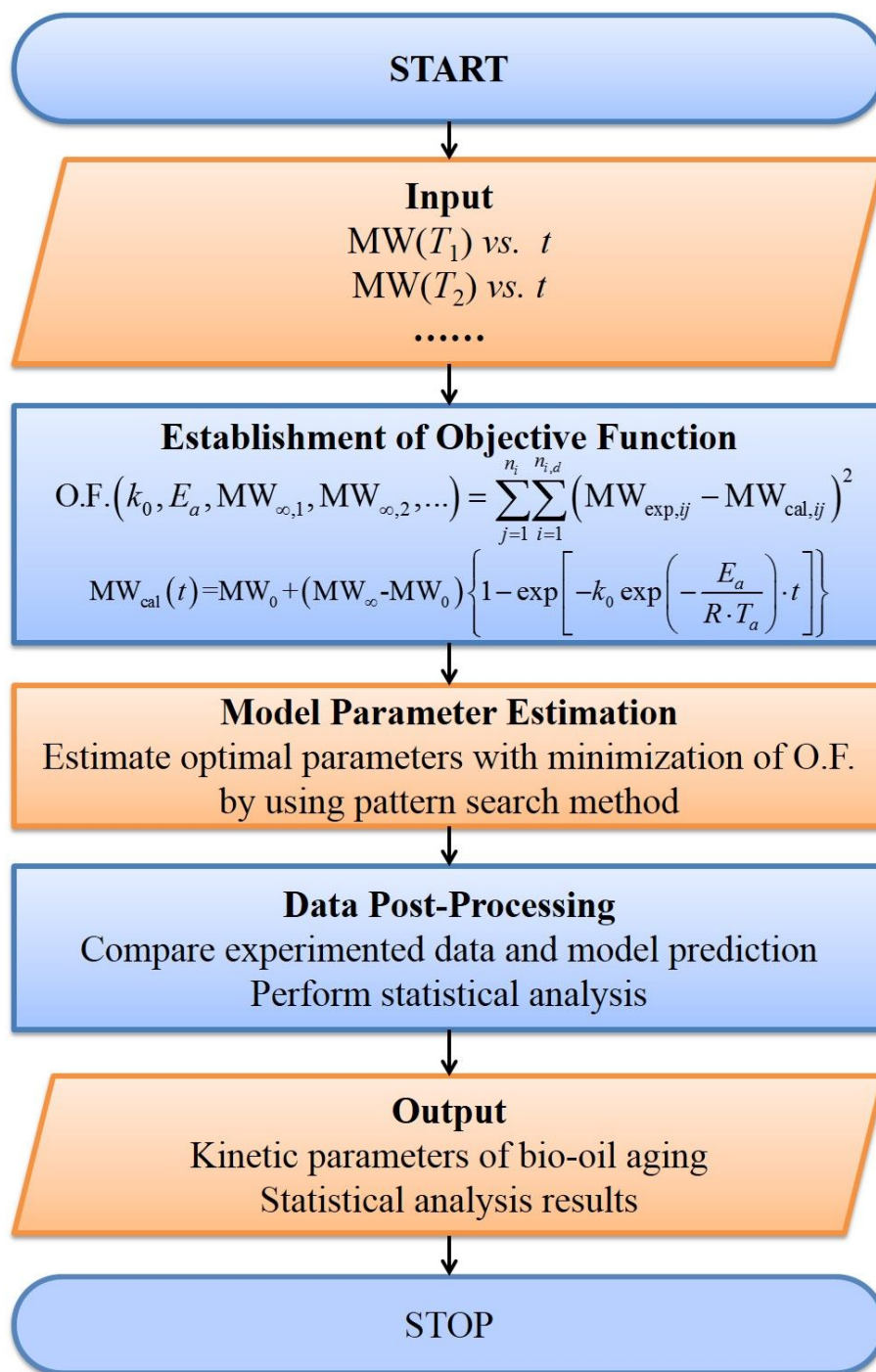


**Figure 1.** Block diagram of advanced procedure for bio-oil aging kinetic modeling

## 5 Results and discussion

### 5.1 Properties of fresh bio-oil

**Table 1** lists the basic properties of bio-oil sample before aging. For comparison, the properties of heavy fuel oil<sup>44</sup> are also included in **Table 1**. From **Table 1**, it can be

obtained that bio-oil contains much higher water content than heavy fuel oil and has a HHV of less than half of heavy fuel oil.

**Table 1.** Physicochemical properties of fresh bio-oil sample and heavy fuel oil

Property	Unit	Bio-oil	Heavy fuel oil <sup>44</sup>
Density	g mL <sup>-1</sup>	1.26 ± 0.02	0.95
Water content	wt.%	12.1 ± 0.6	0.32
pH value		2.87 ± 0.01	
Dynamic viscosity @ 313 K	cP	95.3 ± 0.2	123.5
Higher heating value (HHV)	MJ kg <sup>-1</sup>	17.43 ± 0.24	44.23
Weight-average molecular weight		532.5 ± 15.2	

## 5.2 Changes in water content and viscosity during aging

The water contents for all bio-oil samples increased slightly from 12.1 to 13.2 wt.% as the aging time and temperature increased. The slight increase of water content is caused by some condensation and dehydration reactions <sup>45</sup>.

The changes in bio-oil's viscosity during aging at different temperatures of 303, 333 and 363 K are shown in **Figure 2**. The viscosity of bio-oils was found to gradually increased with aging time and higher aging temperatures favored the increase. This

1  
2  
3  
4 study mainly focused on the aging kinetic analysis on the change in average molecular  
5  
6 weight. The viscosity-based kinetic modeling for bio-oil aging is not considered here  
7  
8  
9 and will be done in our future work.  
10  
11  
12  
13  
14  
15  
16  
17  
18  
19  
20  
21  
22  
23  
24  
25  
26  
27  
28  
29  
30  
31  
32  
33  
34  
35  
36  
37  
38  
39  
40  
41  
42  
43  
44  
45  
46  
47  
48  
49  
50  
51  
52  
53  
54  
55  
56  
57  
58  
59  
60

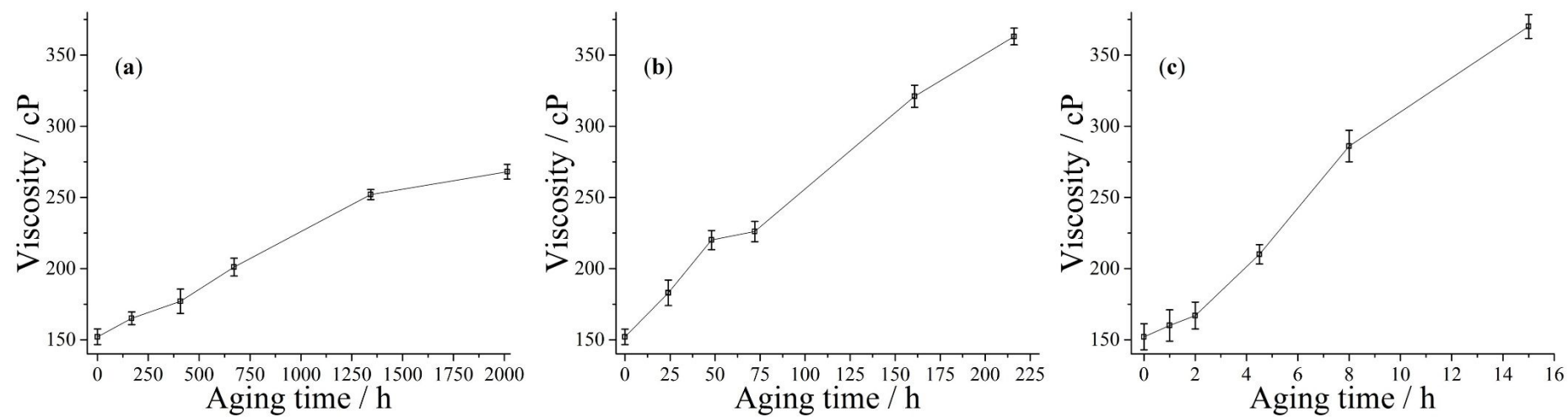


**Figure 2.** Changes in viscosity of bio-oil samples at aging temperatures of (a) 303 K, (b) 333 K, and (c) 363 K

### 5.3 Bio-oil aging kinetic analysis using traditional method

The traditional method of processing experimental kinetic data of bio-oil aging was conducted in this study. The fittings of the aging experimental kinetic data of the bio-oil sample at different temperatures with the kinetic model (2) were performed in DataFit (a powerful tool for nonlinear regression, statistical analysis, and data plotting) and the corresponding aging kinetic parameter values were obtained (as listed in **Table 2**).

**Table 2.** Aging kinetic parameter values at different aging temperatures from the traditional method

$T_a / \text{K}$	$MW_\infty$	$k / \text{s}^{-1}$
303	856.4	$4.8285 \times 10^{-4}$
333	954.3	$9.0011 \times 10^{-3}$
363	1001.8	$9.2882 \times 10^{-2}$

Based on the obtained  $k$  values at different aging temperatures, the  $E_a$  and  $k_0$  values for the aging of the bio-oil sample can be calculated by using Equation (2):  $E_a = 92.479$  kJ mol<sup>-1</sup> and  $k_0 = 28.400$  s<sup>-1</sup>, respectively. The aging kinetic data were reproduced by using the aging kinetic model with the obtained parameter values and the comparison results between the experimental data and the reproduced curves for bio-oil aging at different temperatures are shown in **Figures 2, 3 and 4**. And the percentage root mean square error (PRMSE) was introduced as a quantitative statistical parameter. It is defined as follows <sup>46</sup>:



$$\text{PRMSE} = \frac{\sqrt{\frac{1}{n_d} \sum_{i=1}^{n_d} (\text{MW}_{\text{exp},i} - \text{MW}_{\text{cal},i})^2}}{\overline{\text{MW}_{\text{exp}}}} \times 100\% \quad (7)$$

where  $\overline{\text{MW}_{\text{exp}}}$  is the average value of weight-average molecular weight during aging.

The PRMSE values between the experimental data and the reproduced curves for bio-oil aging at different aging temperatures were listed in **Table 3**. From **Figures 3, 4, and 5** and **Table 3**, it can be easily noticed that there are relatively large deviations between the experimental data and the model predicted data.

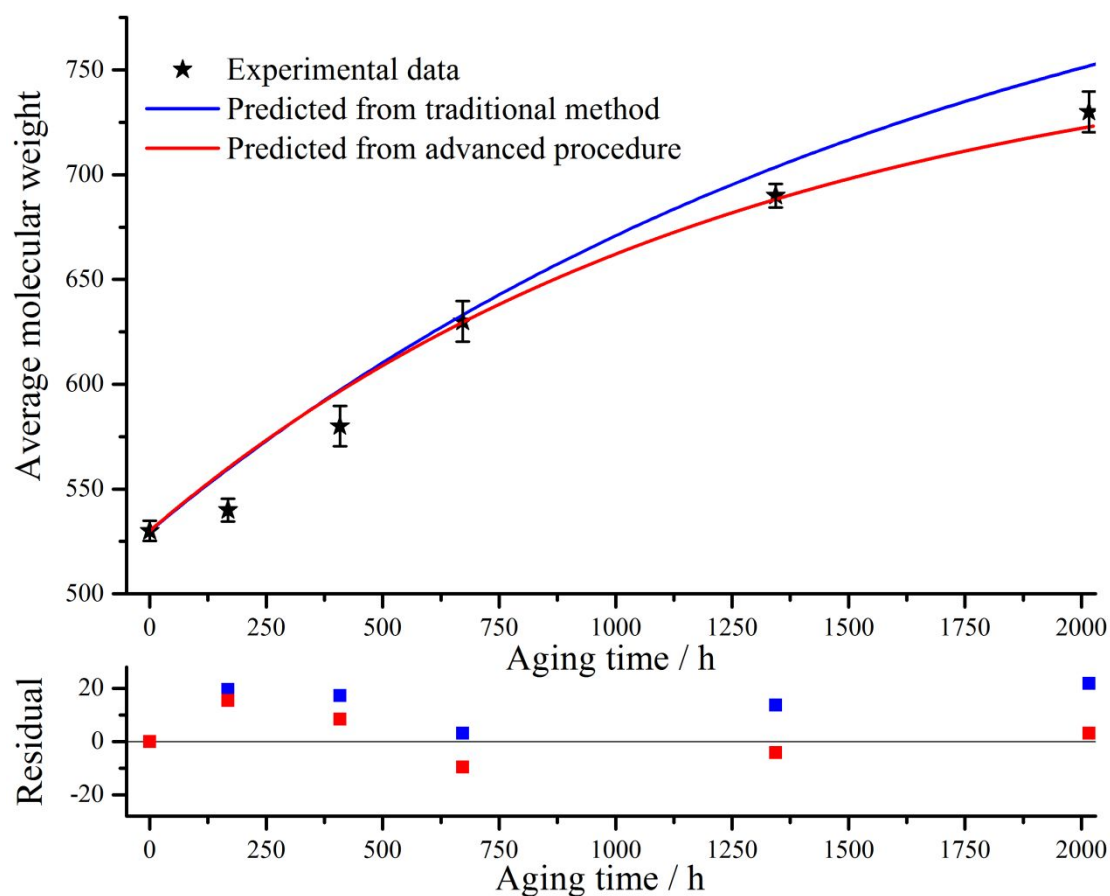


**Figure 3.** Comparison between experimental data and data predicted from the traditional method and advanced procedure for bio-oil aging kinetic analysis at the aging temperature of 303 K

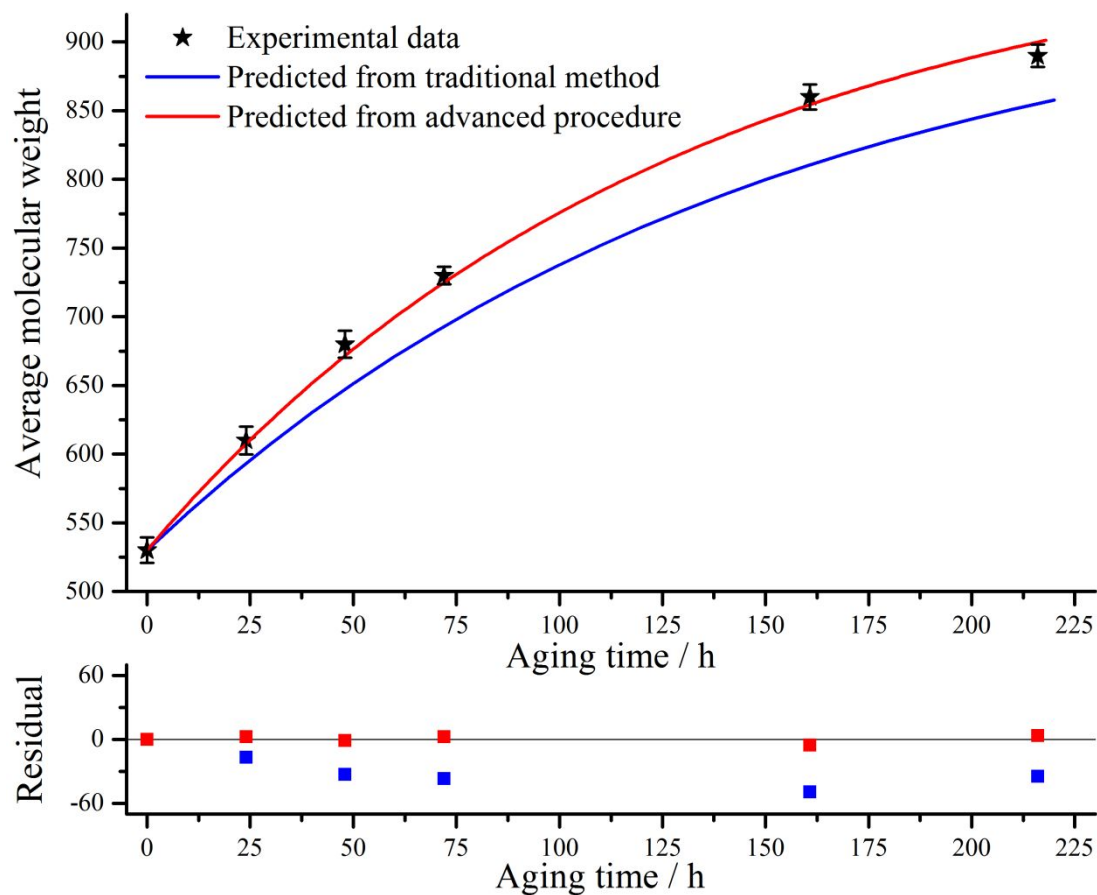


**Figure 4.** Comparison between experimental data and data predicted from the traditional method and advanced procedure for bio-oil aging kinetic analysis at the aging temperature of 333 K

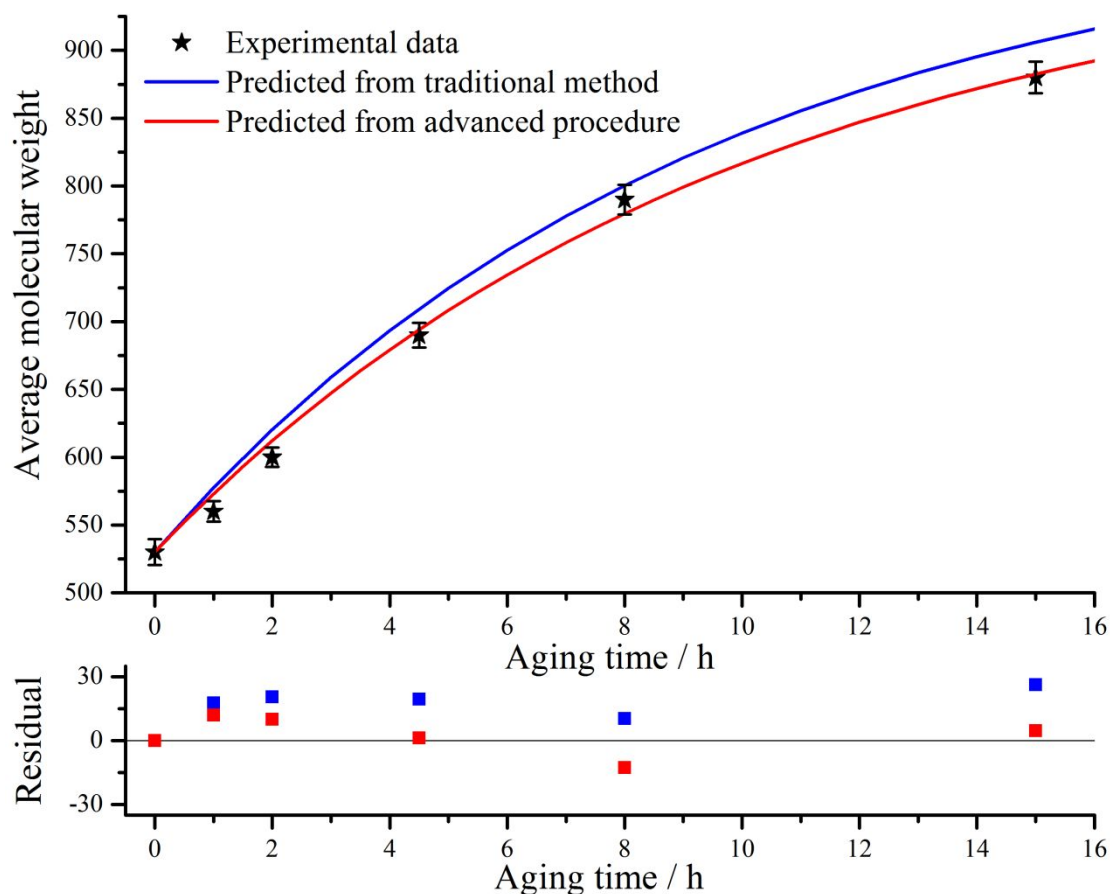


**Figure 5.** Comparison between experimental data and data predicted from the traditional method and advanced procedure for bio-oil aging kinetic analysis at the aging temperature of 363 K

**Table 3.** Aging kinetic parameters for bio-oil aging and corresponding statistical analysis results

Method	$k_0 / s^{-1}$	$E_a / kJ mol^{-1}$	PRMSE		
			@303K	@333K	@363K
Traditional method	28.400	92.478	4.87%	9.11%	5.27%
Advanced procedure	25.990	85.446	1.37%	0.43%	1.24%

#### 5.4 Bio-oil aging kinetic analysis using advanced procedure

1  
2  
3  
4 In order to investigate the effect of  $k_0$  and  $E_a$  values on the objective function (5),  
5  
6 the change of O.F. values calculated for different  $k_0$  and  $E_a$  values ( $k_0 = 12 - 32 \text{ s}^{-1}$  step  
7  
8  $0.01 \text{ s}^{-1}$ ,  $E_a = 74 - 94 \text{ kJ mol}^{-1}$  step  $0.01 \text{ kJ mol}^{-1}$ ) and given  $MW_\infty$  values is shown in  
9  
10 **Figure 6**. As it can be obviously observed in **Figure 6**, the O.F. 3-D scatter plot shows  
11  
12 that there are a certain minimum value and is different for different given  $MW_\infty$  values.  
13  
14 In **Figure 6**, the red 3-D ball represents the minimum point for each set of  $MW_\infty$  values.  
15  
16 Considering the results of above analysis and the complexity of the optimization  
17  
18 problem (6), a certain advanced optimization method needs to be taken into account.  
19  
20  
21  
22  
23  
24  
25  
26  
27  
28  
29  
30  
31  
32  
33  
34  
35  
36  
37  
38  
39  
40  
41  
42  
43  
44  
45  
46  
47  
48  
49  
50  
51  
52  
53  
54  
55  
56  
57  
58  
59  
60

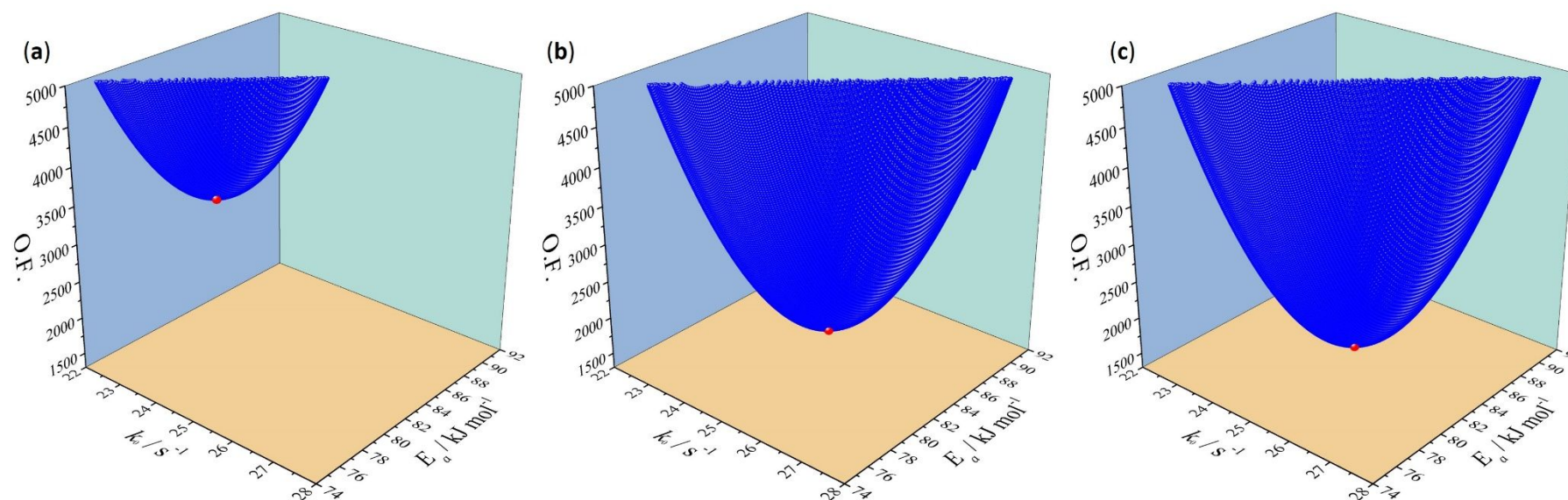


**Figure 6.** Changing of O.F. depending on different  $k_0$  and  $E_a$  values with given  $MW_{\infty}$  values: (a)  $MW_{\infty,1} = 755$ ,  $MW_{\infty,2} = 1055$ ,  $MW_{\infty,3} = 1085$ ;

(b)  $MW_{\infty,1} = 760$ ,  $MW_{\infty,2} = 960$ ,  $MW_{\infty,3} = 990$ ; (c)  $MW_{\infty,1} = 755$ ,  $MW_{\infty,2} = 1055$ ,  $MW_{\infty,3} = 1085$ .

1  
2  
3  
4 As mentioned above, the pattern search method is considered in this study, which  
5  
6 is implemented in the MATLAB software environment. In the beginning of the  
7  
8 implementation of the pattern search method, an initial guess of the aging model  
9  
10 parameters should be given. In this study, the minimum point in **Figure 6(c)** is chosen  
11  
12 as the initial guess for the optimization. **Figure 7** shows the best objective function  
13  
14 value at every iteration, function evaluation numbers per interval and mesh size at every  
15  
16 iteration. The results included in **Figure 7** indicate that the objective function decreases  
17  
18 with iteration. Initially it sharply decreases, then level off.  
19  
20  
21  
22  
23  
24  
25  
26  
27  
28  
29  
30  
31  
32  
33  
34  
35  
36  
37  
38  
39  
40  
41  
42  
43  
44  
45  
46  
47  
48  
49  
50  
51  
52  
53  
54  
55  
56  
57  
58  
59  
60

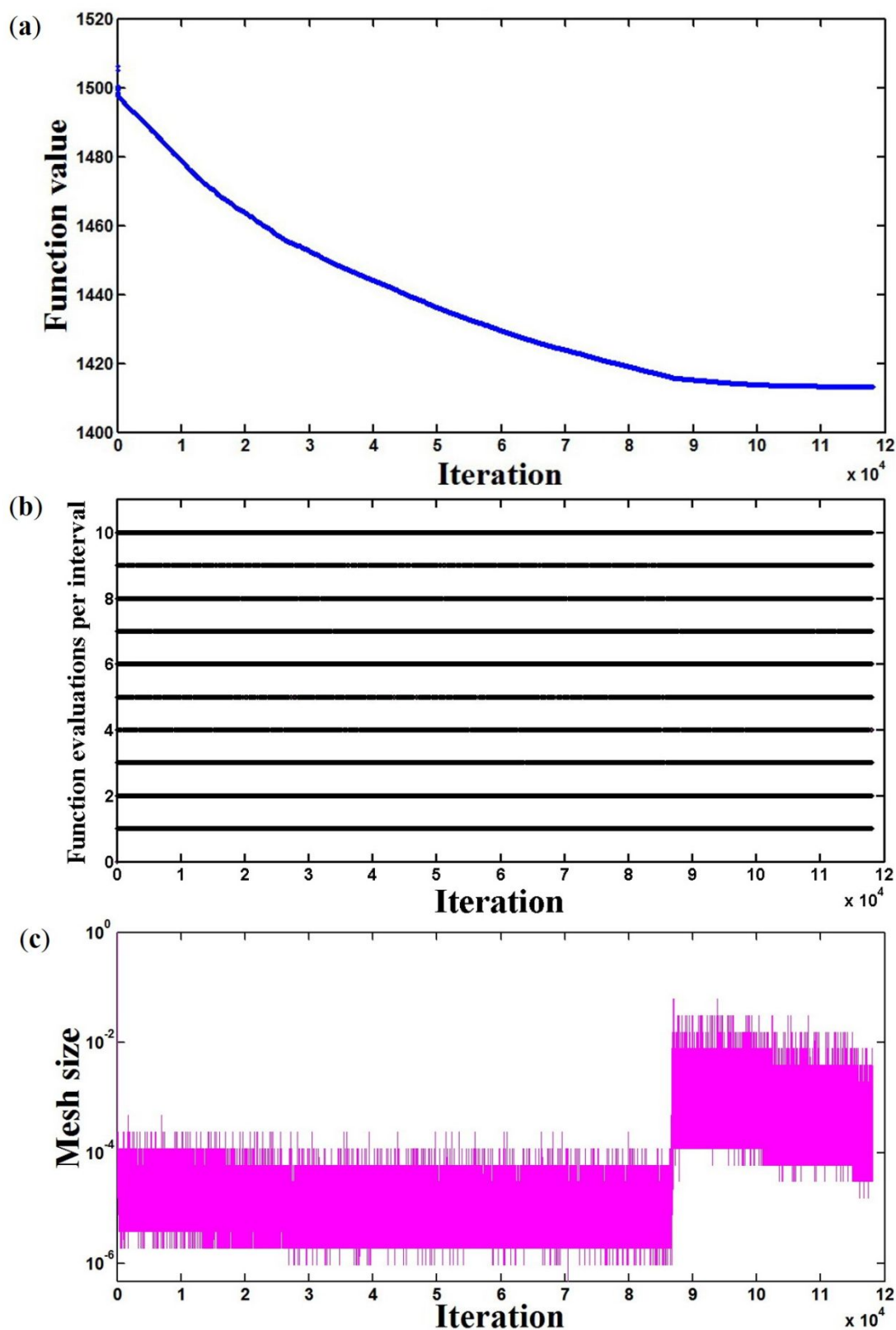


**Figure 7.** (a) Best objective function value at each iteration; (b) Function evaluations per interval; (c) Mesh size at each iteration for optimization calculation using pattern search method

1  
2  
3  
4 The optimized aging kinetic parameters are established by the advanced procedure  
5  
6 and listed in **Table 3**. The comparison of predicted aging kinetic curves with the above  
7  
8 optimized parameters with the experimental data are also shown in **Figures 3, 4, and 5**  
9  
10 for aging temperatures of 303, 333 and 363 K, respectively. The corresponding PRMSE  
11  
12 values between the experimental data and model prediction are listed in **Table 3**. The  
13  
14 results included in **Figures 3, 4, and 5** and **Table 3** demonstrate that the aging kinetic  
15  
16 model (4) can fit the aging experimental data of the bio-oil sample sufficiently well for  
17  
18 all aging temperatures.  
19  
20  
21  
22  
23

24  
25 To evaluate the validity of the comprehensive aging kinetic model, the  
26  
27 experimental data point at aging temperature of 363 K and aging time of 24 h and the  
28  
29 experimental data set at aging temperature of 353 K with aging time ranging from 0 to  
30  
31 60 h, which were not used for the calculation of the aging kinetic parameters, were  
32  
33 compared with the data from the aging kinetic model with the optimized kinetic  
34  
35 parameter. From **Figure 8**, the model prediction describes the experimental data well.  
36  
37 This indicated that the developed model and the obtained kinetic parameters were  
38  
39 effective for describing the aging kinetic behaviors of the bio-oil samples.  
40  
41  
42  
43  
44  
45  
46  
47  
48  
49  
50  
51  
52  
53  
54  
55  
56  
57  
58  
59  
60



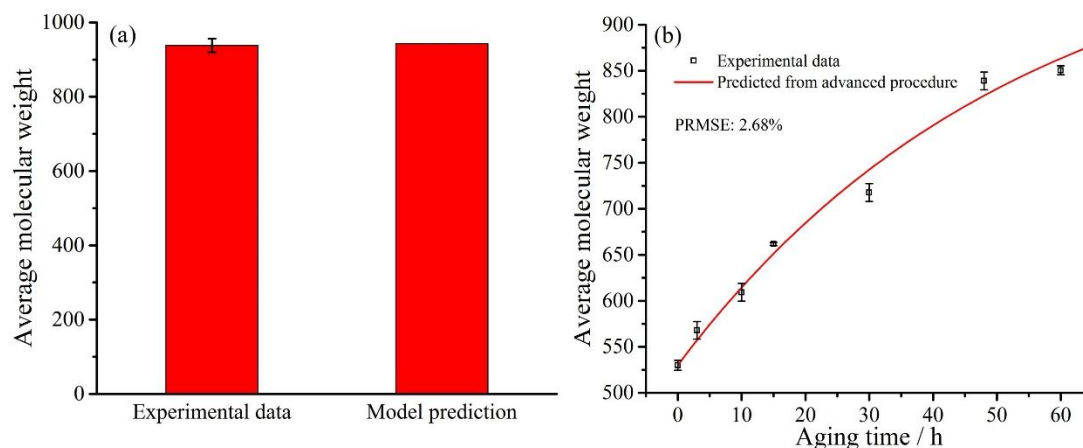


**Figure 8.** Verification of the model prediction usability for bio-oil aging at (a) aging temperature: 363 K, aging time: 24 h; (b) aging temperature: 353 K, aging time: from 0 to 60 h.

The aging kinetic behaviors at interpolated and extrapolated aging temperatures can be predicted by means of the numerical calculations of the aging kinetic model (4) with the optimized aging kinetic parameters. In addition, differentiating the aging kinetic model (4) with respect to  $t$ , the change rate of weight-average molecular weight with the aging time can be obtained (see Equation (8)).

$$\frac{dMW}{dt}(t) = k_0 (MW_\infty - MW_0) \exp\left[-\frac{E_a}{R \cdot T_a} - k_0 \exp\left(-\frac{E_a}{R \cdot T_a}\right) \cdot t\right] \quad (8)$$

**Figure 9** shows the predicted curves of the change and change rate of weight-average molecular weight with the aging time at the interpolated and extrapolated temperatures of 313, 323, 348 and 368 K. From **Figure 9**, it can be obtained that (1) the weight-average molecular weight of the bio-oil sample increases with the aging period, (2) the change and change rate of weight-average molecular weight are greater at higher temperatures (e.g., 348 and 368 K) than those occur at lower temperatures

1  
2  
3  
4 (e.g., 313 and 323 K). The results included in **Figure 9** reveal that weight-average  
5  
6 molecular weight of the bio-oil sample after 60 days of aging at 313 K is equivalent to  
7  
8 that obtained after approximately 278 hours at 323 K, to 27.3 hours at 348 K and to 5.3  
9  
10 hours at 368 K.  
11  
12

13  
14 The weight-average molecular weight of bio-oils significantly increased with  
15  
16 increasing aging time, that indicates the formation of large molecules. And higher  
17  
18 temperatures favor the increase of average molecular weight. The results are in good  
19  
20 agreement with the widely accepted bio-oil aging mechanism that refers the bio-oil  
21  
22 aging is mainly caused by self-condensation reactions and some mutual interactions of  
23  
24 different bio-oil fractions <sup>18, 47</sup>. Those condensation reactions accelerate greatly with  
25  
26 increasing aging temperature <sup>48</sup>.  
27  
28  
29  
30  
31  
32  
33  
34  
35  
36  
37  
38  
39  
40  
41  
42  
43  
44  
45  
46  
47  
48  
49  
50  
51  
52  
53  
54  
55  
56  
57  
58  
59  
60

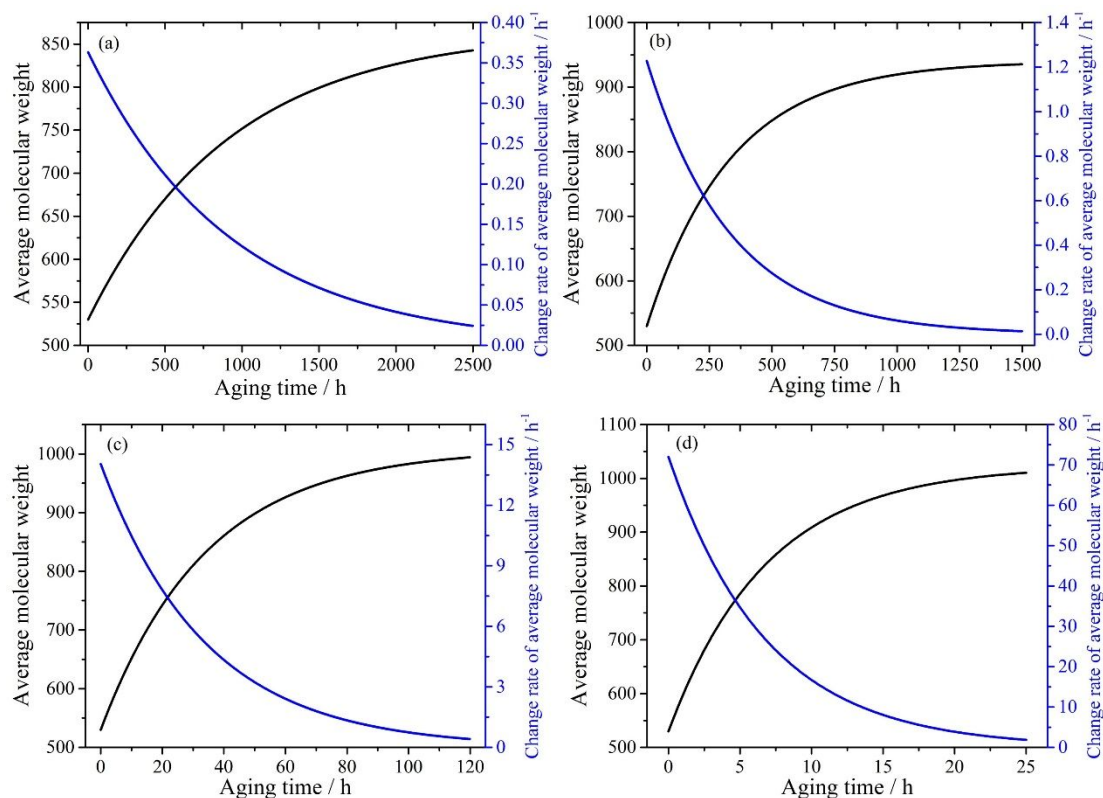


**Figure 9.** Aging kinetic behaviors at aging temperatures of (a) 313 K, (b) 323 K, (c) 348 K and (d) 368 K predicted from comprehensive aging kinetic model with optimized kinetic parameters

## 6 Conclusions

This study focuses on the investigation of bio-oil aging characteristics in terms of change in weight-average molecular weight and performing kinetic modeling of bio-oil aging. The advanced procedure based on the pattern search method has been developed to accurately analyze the kinetic experimental data of bio-oil aging. The following findings and conclusions are drawn: (1) The aging kinetic experiments of the bio-oil sample from poplar wood pyrolysis at different aging temperatures are performed. The change and change rate in the weight-average molecular weight of bio-oil are greater

1  
2  
3  
4 at higher temperatures than those occur at lower temperatures. (2) The aging kinetic  
5  
6 analysis based on the traditional method with two separated fittings can't provide  
7  
8 accurate results. (3) The advanced procedure to process kinetic experimental data of  
9  
10 bio-oil aging has been developed by simultaneously considering all aging temperatures  
11  
12 and using the pattern search method. The results predicted from the comprehensive  
13  
14 aging kinetic model coupled with the optimized kinetic parameters were compared with  
15  
16 the aging kinetic experimental data of bio-oil at different temperatures. The aging  
17  
18 kinetic model with the optimized parameters obtained from the advanced procedure  
19  
20 describes the experimental data at different temperatures more reliable and accurate  
21  
22 than that from the traditional method.  
23  
24  
25  
26  
27  
28  
29  
30  
31

### 32 **Acknowledgements**

33  
34 Financial support from Shanghai Jiao Tong University (Agri-X Project: Co-  
35  
36 pyrolysis of biomass and waste rubber for high-performance bio-bitumen) is greatly  
37  
38 acknowledged. We appreciate the language contributions of Miss Nishu, Ph.D.  
39  
40 candidate from School of Agriculture and Biology, Shanghai Jiao Tong University,  
41  
42 People's Republic of China.  
43  
44  
45  
46  
47  
48

### 49 **References**

- 50  
51 1. Lu, H.; Xu, F.; Liu, H.; Wang, J.; Campbell, D. E.; Ren, H., Energy-based analysis  
52  
53 of the energy security of China. *Energy* **2019**, 181, 123-135.  
54  
55  
56 2. Dorian, J. P., *China's Energy And Mineral Industries: Current Perspectives*. Taylor  
57  
58 & Francis: 2019.  
59  
60

3. Xiu, S.; Shahbazi, A., Bio-oil production and upgrading research: A review. *Renewable and Sustainable Energy Reviews* **2012**, 16, (7), 4406-4414.
4. Lehto, J.; Oasmaa, A.; Solantausta, Y.; Kytö, M.; Chiaramonti, D., Review of fuel oil quality and combustion of fast pyrolysis bio-oils from lignocellulosic biomass. *Applied Energy* **2014**, 116, 178-190.
5. Lyu, G.; Wu, S.; Zhang, H., Estimation and Comparison of Bio-Oil Components from Different Pyrolysis Conditions. *Frontiers in Energy Research* **2015**, 3, (28).
6. Demirbas, A.; Alidrisi, H.; Balubaid, M. A., API gravity, sulfur content, and desulfurization of crude oil. *Petroleum Science and Technology* **2015**, 33, (1), 93-101.
7. Sharifzadeh, M.; Sadeqzadeh, M.; Guo, M.; Borhani, T. N.; Murthy Konda, N. V. S. N.; Garcia, M. C.; Wang, L.; Hallett, J.; Shah, N., The multi-scale challenges of biomass fast pyrolysis and bio-oil upgrading: Review of the state of art and future research directions. *Progress in Energy and Combustion Science* **2019**, 71, 1-80.
8. Hu, X.; Gholizadeh, M., Biomass pyrolysis: A review of the process development and challenges from initial researches up to the commercialisation stage. *Journal of Energy Chemistry* **2019**, 39, 109-143.
9. Ansari, K. B.; Arora, J. S.; Chew, J. W.; Dauenhauer, P. J.; Mushrif, S. H., Fast pyrolysis of cellulose, hemicellulose, and lignin: Effect of operating temperature on bio-oil yield and composition and insights into the intrinsic pyrolysis chemistry. *Industrial & Engineering Chemistry Research* **2019**, 58, (35), 15838-15852.
10. Su, N.; Xiao, F.; Wang, J.; Cong, L.; Amirkhanian, S., Productions and applications of bio-asphalts – A review. *Construction and Building Materials* **2018**, 183, 578-591.

- 1  
2  
3  
4 11. Raman, N. A. A.; Hainin, M. R.; Hassan, N. A.; Ani, F. N., A review on the  
5  
6 application of bio-oil as an additive for asphalt. *Jurnal Teknologi* **2015**, *72*, (5), 105-  
7  
8 110.  
9  
10  
11 12. Tayh, S. A.; Muniandy, R.; Hassim, S.; Jakarni, F.; Aburkaba, E., An overview of  
12  
13 utilization of bio-oil in hot mix asphalt. *WALIA Journal* **2014**, *30*, (S3), 131-141.  
14  
15  
16 13. Yu, J.; Ren, Z.; Gao, Z.; Wu, Q.; Zhu, Z.; Yu, H., Recycled heavy bio oil as  
17  
18 performance enhancer for rubberized bituminous binders. *Polymers* **2019**, *11*, (5).  
19  
20  
21 14. Pinheiro Pires, A. P.; Arauzo, J.; Fonts, I.; Domine, M. E.; Fernández Arroyo, A.;  
22  
23 Garcia-Perez, M. E.; Montoya, J.; Chejne, F.; Pfromm, P.; Garcia-Perez, M.,  
24  
25 Challenges and opportunities for bio-oil refining: A review. *Energy & Fuels* **2019**, *33*,  
26  
27 (6), 4683-4720.  
28  
29  
30 15. Tang, Z.; Lu, Q.; Zhang, Y.; Zhu, X.; Guo, Q., One step bio-oil upgrading through  
31  
32 hydrotreatment, esterification, and cracking. *Industrial & Engineering Chemistry*  
33  
34 *Research* **2009**, *48*, (15), 6923-6929.  
35  
36  
37 16. Yang, Z.; Kumar, A.; Huhnke, R. L., Review of recent developments to improve  
38  
39 storage and transportation stability of bio-oil. *Renewable and Sustainable Energy*  
40  
41 *Reviews* **2015**, *50*, 859-870.  
42  
43  
44 17. Chen, D.; Zhou, J.; Zhang, Q.; Zhu, X., Evaluation methods and research  
45  
46 progresses in bio-oil storage stability. *Renewable and Sustainable Energy Reviews*  
47  
48 **2014**, *40*, 69-79.  
49  
50  
51 18. Oasmaa, A.; Fonts, I.; Pelaez-Samaniego, M. R.; Garcia-Perez, M. E.; Garcia-  
52  
53 Perez, M., Pyrolysis oil multiphase behavior and phase stability: A review. *Energy &*  
54  
55  
56  
57  
58  
59  
60

1  
2  
3  
4 *Fuels* **2016**, 30, (8), 6179-6200.  
5

6  
7 19. Zhang, M.; Li, M.; Wu, H., Ageing of bio-oil and its fractions in presence of  
8  
9 surfactants. *Fuel* **2019**, 252, 403-407.  
10

11  
12 20. Haverly, M. R.; Okoren, K. V.; Brown, R. C., Thermal stability of fractionated bio-  
13  
14 oil from fast pyrolysis. *Energy & Fuels* **2016**, 30, (11), 9419-9426.  
15

16  
17 21. Kaya, D.; Topal, A.; McNally, T., Relationship between processing parameters and  
18  
19 aging with the rheological behaviour of SBS modified bitumen. *Construction and*  
20  
21 *Building Materials* **2019**, 221, 345-350.  
22

23  
24 22. Luo, X.; Gu, F.; Zhang, Y.; Lytton, R. L.; Birgisson, B., Kinetics-based aging  
25  
26 evaluation of in-service recycled asphalt pavement. *Journal of Cleaner Production*  
27  
28 **2018**, 200, 934-944.  
29

30  
31 23. Yang, Y.; Zhang, Y.; Omairey, E.; Cai, J.; Gu, F.; Bridgwater, A. V., Intermediate  
32  
33 pyrolysis of organic fraction of municipal solid waste and rheological study of the  
34  
35 pyrolysis oil for potential use as bio-bitumen. *Journal of Cleaner Production* **2018**, 187,  
36  
37 390-399.  
38

39  
40 24. Sun, Z.; Yi, J.; Feng, D.; Kasbergen, C.; Scarpas, A.; Zhu, Y., Preparation of bio-  
41  
42 bitumen by bio-oil based on free radical polymerization and production process  
43  
44 optimization. *Journal of Cleaner Production* **2018**, 189, 21-29.  
45  
46

47  
48 25. Nolte, M. W.; Liberatore, M. W., Real-time viscosity measurements during the  
49  
50 accelerated aging of biomass pyrolysis oil. *Energy & Fuels* **2011**, 25, (7), 3314-3317.  
51  
52

53  
54 26. Oasmaa, A.; Kuoppala, E., Fast pyrolysis of forestry residue. 3. Storage stability  
55  
56 of liquid fuel. *Energy & Fuels* **2003**, 17, (4), 1075-1084.  
57  
58  
59  
60

- 1  
2  
3  
4 27. Oasmaa, A.; Korhonen, J.; Kuoppala, E., An approach for stability measurement  
5  
6 of wood-based fast pyrolysis bio-oils. *Energy & Fuels* **2011**, *25*, (7), 3307-3313.  
7  
8  
9 28. Chai, M.; He, Y.; Nishu; Sun, C.; Liu, R., Effect of fractional condensers on  
10  
11 characteristics, compounds distribution and phenols selection of bio-oil from pine  
12  
13 sawdust fast pyrolysis. *Journal of the Energy Institute* **2019**, doi:  
14  
15 10.1016/j.joei.2019.05.001.  
16  
17  
18 29. Cai, J.; Banks, S. W.; Yang, Y.; Darbar, S.; Bridgwater, T., Viscosity of aged bio-  
19  
20 oils from fast pyrolysis of beech wood and miscanthus: Shear rate and temperature  
21  
22 dependence. *Energy & Fuels* **2016**, *30*, (6), 4999-5004.  
23  
24  
25 30. Elliott, D. C.; Oasmaa, A.; Preto, F.; Meier, D.; Bridgwater, A. V., Results of the  
26  
27 IEA Round Robin on Viscosity and Stability of Fast Pyrolysis Bio-oils. *Energy & Fuels*  
28  
29 **2012**, *26*, (6), 3769-3776.  
30  
31  
32 31. Garcia-Perez, M.; Chaala, A.; Pakdel, H.; Kretschmer, D.; Roy, C.,  
33  
34 Characterization of bio-oils in chemical families. *Biomass and Bioenergy* **2007**, *31*, (4),  
35  
36 222-242.  
37  
38  
39 32. Tadanier, C. J.; Berry, D. F.; Knocke, W. R., Dissolved organic matter apparent  
40  
41 molecular weight distribution and number-average apparent molecular weight by batch  
42  
43 ultrafiltration. *Environmental Science & Technology* **2000**, *34*, (11), 2348-2353.  
44  
45  
46 33. Harman-Ware, A. E.; Ferrell, J. R., Methods and challenges in the determination  
47  
48 of molecular weight metrics of bio-oils. *Energy & Fuels* **2018**, *32*, (9), 8905-8920.  
49  
50  
51 34. Lazzari, E.; Schena, T.; Marcelo, M. C. A.; Primaz, C. T.; Silva, A. N.; Ferrão, M.  
52  
53 F.; Bjerck, T.; Caramão, E. B., Classification of biomass through their pyrolytic bio-oil  
54  
55  
56  
57  
58  
59  
60



1  
2  
3  
4 composition using FTIR and PCA analysis. *Industrial Crops and Products* **2018**, 111,  
5  
6 856-864.

7  
8  
9 35. Mohan, D.; Pittman, C. U.; Steele, P. H., Pyrolysis of Wood/Biomass for Bio-oil:  
10  
11 A Critical Review. *Energy & Fuels* **2006**, 20, (3), 848-889.

12  
13  
14 36. Kim, T.-S.; Kim, J.-Y.; Kim, K.-H.; Lee, S.; Choi, D.; Choi, I.-G.; Choi, J. W., The  
15  
16 effect of storage duration on bio-oil properties. *Journal of Analytical and Applied*  
17  
18 *Pyrolysis* **2012**, 95, 118-125.

19  
20  
21 37. Czernik, S.; Johnson, D. K.; Black, S., Stability of wood fast pyrolysis oil. *Biomass*  
22  
23 *and Bioenergy* **1994**, 7, (1), 187-192.

24  
25  
26 38. Waterhouse, A. L.; Sacks, G. L.; Jeffery, D. W., Topics Related to Aging. In  
27  
28 *Understanding Wine Chemistry*, Wiley: 2016; pp 294-317.

29  
30  
31 39. Ding, Y.; Zhang, W.; Yu, L.; Lu, K., The accuracy and efficiency of GA and PSO  
32  
33 optimization schemes on estimating reaction kinetic parameters of biomass pyrolysis.  
34  
35 *Energy* **2019**, 176, 582-588.

36  
37  
38 40. Beigi, A. M.; Maroosi, A., Parameter identification for solar cells and module using  
39  
40 a Hybrid Firefly and Pattern Search Algorithms. *Solar Energy* **2018**, 171, 435-446.

41  
42  
43 41. Cai, J.; Ji, L., Pattern search method for determination of daem kinetic parameters  
44  
45 from nonisothermal tga data of biomass. *Journal of Mathematical Chemistry* **2007**, 42,  
46  
47 (3), 547-553.

48  
49  
50 42. Xu, D.; Chai, M.; Dong, Z.; Rahman, M. M.; Yu, X.; Cai, J., Kinetic compensation  
51  
52 effect in logistic distributed activation energy model for lignocellulosic biomass  
53  
54 pyrolysis. *Bioresource Technology* **2018**, 265, 139-145.

- 1  
2  
3  
4 43. Narang, N.; Sharma, E.; Dhillon, J. S., Combined heat and power economic  
5  
6 dispatch using integrated civilized swarm optimization and Powell's pattern search  
7  
8 method. *Applied Soft Computing* **2017**, *52*, 190-202.  
9  
10  
11 44. Hou, S. S.; Huang, W. C.; Rizal, F. M.; Lin, T. H., Co-firing of fast pyrolysis bio-  
12  
13 oil and heavy fuel oil in a 300-kWth furnace. *Applied Sciences (Switzerland)* **2016**, *6*,  
14  
15 (11).  
16  
17  
18 45. Wang, C.; Ding, H.; Zhang, Y.; Zhu, X., Analysis of property variation and stability  
19  
20 on the aging of bio-oil from fractional condensation. *Renewable Energy* **2019**, doi:  
21  
22 10.1016/j.renene.2019.10.159.  
23  
24  
25 46. Patience, G. S., Chapter 2 - Measurement and Analysis. In *Experimental Methods*  
26  
27 *and Instrumentation for Chemical Engineers (Second Edition)*, Patience, G. S., Ed.  
28  
29 Elsevier: 2018; pp 17-63.  
30  
31  
32 47. Meng, J.; Moore, A.; Tilotta, D.; Kelley, S.; Park, S., Toward understanding of bio-  
33  
34 oil aging: Accelerated aging of bio-oil fractions. *ACS Sustainable Chemistry &*  
35  
36 *Engineering* **2014**, *2*, (8), 2011-2018.  
37  
38  
39 48. Hu, X.; Wang, Y.; Mourant, D.; Gunawan, R.; Lievens, C.; Chaiwat, W.;  
40  
41 Gholizadeh, M.; Wu, L.; Li, X.; Li, C.-Z., Polymerization on heating up of bio-oil: A  
42  
43 model compound study. *AIChE Journal* **2013**, *59*, (3), 888-900.  
44  
45  
46  
47  
48  
49  
50  
51  
52  
53  
54  
55  
56  
57  
58  
59  
60